Bounce harmonic Landau damping of plasma waves

F. Anderegg,[a] M. Affolter, A. A. Kabantsev, D. H. E. Dubin, A. Ashourvan, and C. F. Driscoll
Physics Department, University of California San Diego, La Jolla, California 92093, USA

(Received 1 December 2015; accepted 29 February 2016; published online 15 April 2016)

We present measurements of bounce harmonic Landau damping due to z-variations in the plasma potential, created by an azimuthally symmetric "squeeze" voltage V_s applied to the cylindrical wall. Traditional Landau damping on spatially uniform plasma is weak in regimes where the wave phase velocity $v_{ph} \equiv \omega/k$ is large compared to the thermal velocity. However, z-variations in plasma density and potential create higher spatial harmonics, which enable resonant wave damping by particles with bounce-averaged velocities v_{ph}/n, where n is an integer. In our geometry, the applied squeeze predominantly generates a resonance at $v_{ph}/3$. Wave-coherent laser induced fluorescence measurements of particle velocities show a distinctive Landau damping signature at $v_{ph}/3$, with amplitude proportional to the applied V_s. The measured (small amplitude) wave damping is then proportional to V_s^2, in quantitative agreement with theory over a range of 20 in temperature. Significant questions remain regarding "background" bounce harmonic damping due to ubiquitous confinement fields and regarding the saturation of this damping at large wave amplitudes. *Published by AIP Publishing.* [http://dx.doi.org/10.1063/1.4946021]

I. INTRODUCTION

Wave damping by particles bouncing at sub-multiples of the wave frequency was proposed 4 decades ago by Berk and Book[1] and studied theoretically by numerous authors.[2–5] Whenever a mode frequency is close to a multiple of a particle bounce frequency, wave and particles can interact strongly. Typically, in a magnetic mirror device, the electron bounce frequency is close to a multiple of the ion cyclotron frequency, resulting in bounce harmonic damping (or growth). Bounce resonance Landau damping has been observed through the reduction of drift cyclotron loss-cone instability in a mirror plasma at frequencies corresponding to calculated predictions of bounce resonance Landau damping.[6] In the earth magnetosphere, particles can be trapped by mirror fields and perform mirror oscillations near the minimum of the magnetic field, so bounce resonant wave-particle interactions must be included when calculating wave damping.[7] Temporal harmonics due to particles bounce resonance has been observed previously through resonant particle heating in non-neutral plasmas[8] and low pressure inductive plasmas.[9]

Here, we present damping measurements of axisymmetric Trivelpiece-Gould plasma modes in pure ion and pure electron plasmas with enhanced mode damping from a controlled azimuthally symmetric squeeze potential. Coherent Laser Induced Fluorescence (LIF) measurements identify the perturbation of the distribution function from the bounce harmonics particles resonance. The enhanced damping of small amplitude waves due to the applied squeeze is in quantitative agreement with theory.

In general, end confining potentials and small uncontrolled axial potentials are common in Penning-Malmberg traps due to trap imperfections and may contribute to damping of plasma modes. In this paper, we quantify the magnitude of the damping created by a squeeze potential. We apply a squeeze potential V_s to a cylindrical electrode creating inside the plasma an axial barrier $e\varphi_s(r)$ small compared to the average thermal energy T of plasma particles. While the squeeze potential can cause particles to be locally trapped in a potential minimum on either side of the squeeze, the effect of trapped particles is negligible for axisymmetric waves with $e\varphi_s/T \ll 1$. For non-axisymmetric waves, trapped-particle-mediated effects due to externally applied squeeze have been previously reported.[10]

According to theory,[11] the squeeze modifies the equilibrium density and potential, thus modifying the orbits of the particles, and modifies the spatial form of the mode potential. Particles moving in z experience a non-sinusoidal mode potential caused by the squeeze, producing harmonics of the mode potential at multiples of the particles bounce frequency that are Landau damped, even when regular Landau damping is negligible since the mode phase velocity is large compared to the thermal speed.

More precisely, particles are bouncing in the trap at bounce frequency $f_b(r,E)$ which depend on their energy and radial location. Bounce harmonic Landau damping occurs when a multiple of the bounce frequency is commensurate with the wave frequency, that is,

$$n f_b(r,E) = f_{wave}. \tag{1}$$

Here, n represents the Fourier time harmonic of the potential as seen by a particle moving through the wave; $n = 1$ corresponds to regular Landau damping and $n > 1$ produces the bounce harmonic damping of interest here. The radial dependence of the bounce frequency is due to the fact that the squeeze potential in the plasma depends on radius and that the plasma length is also a function of radius. Therefore, the resonance condition for bounce harmonics Landau damping is satisfied at different radii by particles having slightly different energies.

Note: Paper NI2 4, Bull. Am. Phys. Soc. **60**, 213 (2015).
[a]Invited speaker.

II. BOUNCE-HARMONICS LANDAU DAMPING OF TRIVELPIECE-GOULD WAVES

Trivelpiece-Gould waves[12] are plasma waves with shielding from a conductive cylindrical wall, causing frequencies below the plasma frequency f_p. The modes are treated as standing waves in a periodic system of length L_p, with wavenumber k_z and frequency f_{TG}. According to fluid theory, azimuthally symmetric standing plasma waves in a cylindrical plasma have the following dispersion relation:

$$f_{TG} = f_p \frac{k_z}{\sqrt{k_z^2 + k_\perp^2}} \left[1 + \frac{3}{2}\left(\frac{\bar{v}}{v_{ph}}\right)^2\right]. \tag{2}$$

In a trapped plasma, the standing plasma waves have to "fit" within the plasma dimension and therefore

$$k_z = \frac{m_z \pi}{L_p}, \tag{3}$$

where m_z represents the number of "half-wavelength" in the plasma. These plasma waves have phase velocity $v_{ph} = 2\pi f_{TG}/k_z$, which is aligned with the magnetic field and the axis of the trap. The wave vector $k_\perp$ is a theoretical construct representing the effect of the conducting wall reducing the parallel electric field and therefore reducing the frequency of the wave below the plasma frequency f_p. For a long and thin plasma, $k_\perp$ can be approximated by

$$k_\perp \cong \frac{\sqrt{2}}{R_p}\left[\ln\frac{R_W}{R_p}\right]^{-\frac{1}{2}}. \tag{4}$$

The exact $k_\perp$ is given by a complicated ratio of Bessel function, resulting from the requirement that the potential vanish at the conducting wall.[12,13]

In this paper, we consider the $m_z = 1$ mode, that is, the standing wave with half a wavelength in the plasma column. Thus, for no squeeze, the wave potential has the approximate form

$$\delta\phi(r,z,t) = A_{m_z}(r)\,\cos(m_z \pi z/L_p)\,\cos(2\pi f t). \tag{5}$$

Here, we are ignoring end effects. When a squeeze is added, the equilibrium plasma density and wave potential are modified, taking the more general form

$$\delta n_0(r,z) = \sum_m B_m(r)\,\cos(m\pi z/L_p), \tag{6}$$

and

$$\delta\phi(r,z,t) = \sum_m A_m(r)\,\cos(m\pi z/L_p)\,\cos(2\pi f t). \tag{7}$$

Bounce harmonic Landau damping arises from the resonant interaction of bouncing particles with this wave potential. Since particles are trapped in the plasma, their motion $z(t)$ is periodic in time with frequency $f_b(r,E)$ where E is the particle's energy. The time dependence of the wave potential as seen by the particle is therefore a sum of Fourier harmonics at multiples of the bounce frequency, multiplied by $\cos(2\pi f t)$

$$\delta\phi(r,z(t),t) = \cos(2\pi f t)\sum_m A_m(r)\sum_n \phi_{m,n}(r,E) \times \exp[2\pi i n f_b(r,E)\,t], \tag{8}$$

where $\phi_{m,n}(r,E) = f_b \oint dt \exp(-2\pi i n f_b)\,\cos(m\pi z(t)/L_p)$ is the Fourier time harmonic of the wave potential caused by the particles periodic motion through the mth spatial Fourier harmonic of the wave. Now, whenever a particle is in resonance with the wave, i.e., whenever $\delta\phi(r,z(t),t)$ becomes time-independent, a resonant transfer of wave energy can occur between the particles and the wave, causing wave damping (or growth). From Eq. (8), this resonance occurs whenever $n f_b(r,E) = f$, which reproduces Eq. (1) in the simplest model of Landau damping with no squeeze added only the $n = m_z$ and $m = m_z$ harmonic appears, because particles are assumed to execute specular reflections between flat ends a distance L_p apart; i.e., only ϕ_{m_z,m_z} and $\phi_{m_z,-m_z}$ are nonzero. However, when a static squeeze potential is added, both the particle orbit $z(t)$ and the wave potential $\delta\phi$ are modified, both adding extra Fourier time harmonics to the wave potential experienced by the particle. In general, $\phi_{m,n}$ may be nonzero for any m and n, so bounce harmonic Landau damping may occur for all $n > 0$ in Eq.(8). However, for a wave with odd m_z and a squeeze that is symmetric about the center of the trap, $\phi_{m,n}$ is nonzero only for m and n odd. Thus, for the present experimental conditions with $m_z = 1$, $n = 1$, and $n = 3$ are the dominant bounce-harmonic resonances. However, the conditions are such that $n = 1$ in Eq. (1) requires particle energies well beyond the thermal spread, so $n = 3$ dominates.

III. EXPERIMENTS

We use a Penning-Malmberg trap to confine a magnesium ion plasma in a magnetic field $B = 3$ T.[14] Figure 1 shows a schematic of the cylindrical electrodes with wall radius $R_W = 2.86$ cm, which are contained in ultrahigh vacuum at $P \sim 10^{-10}$ Torr. The typical plasma has a length $10\,\text{cm} < L_p < 14\,\text{cm}$, a radius $R_p \simeq 0.5$cm, and a density $n_0 \simeq 2 \times 10^7 \text{cm}^{-3}$. The temperature is controlled by laser cooling with a parallel beam, in the range of $10^{-4}\,\text{eV} < T < 0.7\,\text{eV}$, resulting in thermal velocities $\bar{v}\,(\text{m/s}) = 2000 \times T_{\text{eV}}^{\frac{1}{2}}$. The plasma is confined in steady state with the use of a weak rotating-wall perturbation.[15] Just before exciting the plasma wave, the rotating wall is turned off for 100 ms.

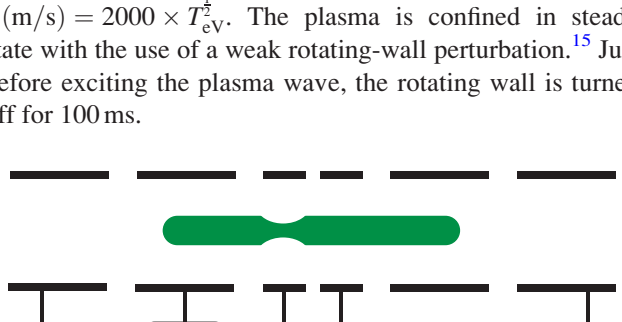

FIG. 1. Non-neutral plasma in Penning-Malmberg trap with controlled squeeze.

Trivelpiece-Gould modes are excited by a burst of 20 cycles with a carefully rounded amplitude envelope to avoid exciting unwanted higher frequency modes. The waves are detected with a separate electrode, and a typical gain of 80 dB is applied to the wall signal before being digitized. The waves have a typical frequency $f \simeq 23.\text{kHz}$, and a typical initial amplitude $\delta n/n \sim 0.3\%$. These standing waves have wavelength $\lambda \simeq 2L_p$. The squeeze voltage is ramped up in 2 ms beginning 10 ms after the wave is excited and is kept constant at V_s for 8 ms before being ramped down in 2 ms. The digitized wall signal is analyzed in short segment of 0.5 ms (corresponding to ~10 cycles of the wave) each segment is fit to a sine wave of frequency f and amplitude $\mathcal{A}$.

The raw wall signal and the amplitude of a large amplitude Trivelpiece-Gould wave (initial $\delta n/n \sim 1\%$) are plotted in Figure 2. The damping rate before the squeeze potential is applied is $\gamma_0 = 15\text{s}^{-1}$ and increases to $\gamma = 70\text{s}^{-1}$ in the presence of a squeeze voltage $V_s = 1.5$ V. Once the squeeze is removed, the damping is $\gamma = 17\text{s}^{-1}$ indicating that the plasma was not strongly modified by the wave and squeeze processes.

Figure 3 presents an overview of the base plasma wave damping γ_0 over 4 decades in temperature. At high temperatures ($T \sim 1$ eV), Landau damping dominates. Quantitative agreement with Landau theory is obtained for small amplitude waves; and nonlinear particle trapping is observed for larger amplitude waves. At lower temperatures ($T \sim 0.1$ eV), typical Landau damping becomes exponentially weak; but the similar Landau interaction can occur with harmonics of the wave presumably created by plasma end effects. In this paper, we increase the amount of harmonics by applying an external squeeze voltage to the plasma. At cryogenic temperatures (10^{-3} eV), collisions with impurity species cause a

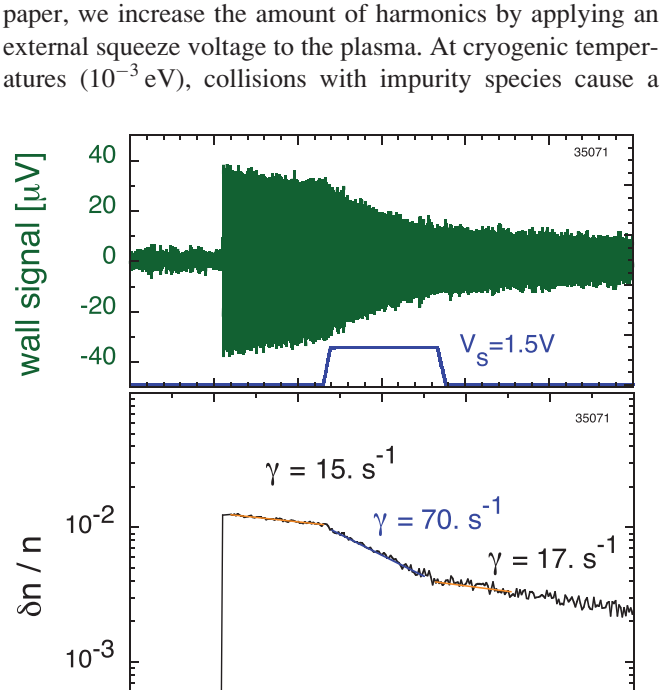

FIG. 2. Wall signal evolution and corresponding wave amplitude, when an external squeeze potential is applied.

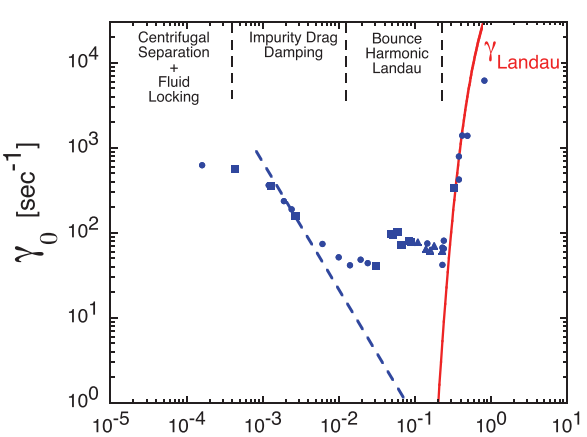

FIG. 3. Plasma wave damping versus temperature before application of squeeze voltage.

"drag" on the majority species, which directly damps the wave motions. This drag is enhanced by an order of magnitude by the newly analyzed long-range collisional slowing.[16] At ultra-low temperatures, the various species become separated radially due to centrifugal effects, and the drag damping is observed to decrease. The dashed line is a theoretical prediction of impurity drag damping scaling with collisionality as $T^{-3/2}$. In the temperature range of bounce harmonic Landau damping, drag damping is weak.

Figure 4 shows the measured damping plotted against the squeeze voltage for a plasma at $T = 0.07$ eV. The open square symbols are the measured damping γ_0 before the squeeze is applied. The damping rate increases by one order of magnitude when a squeeze of $V_s = 4.\text{V}$ is applied. The base damping γ_0 comes from several damping processes including instrumental damping, collisional drag damping, bounce harmonic Landau damping from plasma ends, and Landau damping at higher temperatures. The measured damping is written as

$$\gamma = \gamma_0 + \gamma_s, \tag{9}$$

where γ_s is presumed to have the following form:

$$\gamma_s = a_2 V_s^2, \tag{10}$$

that is, the squeeze damping increases as the square of the squeeze voltage V_s. In Figure 4, the dashed line is a quadratic

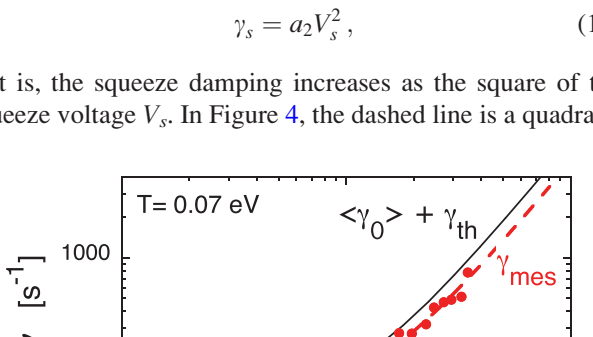

FIG. 4. Damping vs squeeze voltage. The solid line is the theory prediction from Ref. 11, and the dashed line is a quadratic fit to the data.

fit to the data, with $\gamma(s^{-1}) = 83 + 52V_s^2$, where V_s has units of volts. The solid line in Figure 4 is the bounce harmonic Landau damping theory prediction from Equation (218) of Ref. 11 with no adjustable parameters added to the measured base damping.

Positive V_s are effectively "squeezing" the ion plasma radially, in contrast, negative V_s are "anti-squeezing" it. In both cases, the externally applied potential is modifying the orbit of some particles and introducing bounce harmonics in the system. As shown in Figure 5, the damping increases as V_s^2 for both a positive and negative squeeze, as to be expected from simple examination of Equation (106) of Ref. 11. Furthermore, the coefficient a_2 appears to be similar for positive and negative V_s, demonstrating that trapped particles do not participate in the damping mechanism. For the data presented in Figure 5, the plasma temperature is $T = 0.058$ eV and the mode frequency in the absence of squeeze is 20.98 kHz. The dashed line in Figure 5 is a fit giving $\gamma(s^{-1}) = 34 + 56.3\,V_s^2$. The solid line is the theory prediction from Equation (218) of Ref. 11 giving $a_2 = 50.0$, added to the measured base damping γ_0.

Also shown in Figure 5 is the change of wave frequency due to external squeeze. The frequency shift $\Delta f/f$ is about 2% for $V_s = 1$. V. A positive squeeze reduces the frequency of the wave and a negative squeeze increases the frequency. This is because a positive (negative) squeeze potential applied close to the center of the column decreases (increases) the number of particles where the axial electric field of wave is large, and therefore, decreases (increases) the frequency of the wave. A second contribution to the frequency shift comes from plasma length changes due to the applied squeeze potential. The solid line is a theoretical prediction from Equation (70) of Ref. 11 which neglects length changes. The theory predicts the frequency shift correctly within 12%. A theory that includes plasma length changes is currently under development.

Figure 6 shows the damping rate $\gamma - \gamma_0$ plotted versus the applied squeeze voltage V_s for various ion plasma temperatures and also one electron plasma. Electron plasmas are confined in a different apparatus ($B = 0.2$ T, $L_p = 48$ cm, $R_p = 1.2$ cm, $n_0 = 1.3 \times 10^7\,\mathrm{cm}^{-3}$, and $T = 1$ eV). In this device, the lowest order Trivelpiece-Gould mode is at a frequency of 2.1 MHz. Electron plasmas exhibit the same damping behavior. The solid lines in Figure 6 are prediction from Equation (218) of Ref. 11 with no adjustable parameters. At lower temperature, squeeze damping is weaker since the squeeze potential applied to the electrode is more shielded due to increased Debye screening, and also the Maxwellian distribution has less particles at the phase velocity of a given bounce harmonic.

The Bounce harmonic theory[11] assumes that the particles bounce frequency f_b is larger than the ion-ion collision-rate $\nu_{ii} = 16/15\sqrt{\pi} n_0 \bar{v} b^2 \ln(r_c/b)$. For our experimental conditions (Mg^+ and $n_0 = 2 \times 10^7 \mathrm{cm}^{-3}, B = 3\mathrm{T}$), $f_b > \nu_{ii}$ for $T > 0.014$eV. Experimentally one observes that even when $f_b < \nu_{ii}$ plasma modes are still damped by the presence of an azimuthal squeeze potential and the squeeze damping appears to be smaller but is still proportional to V_s^2, possibly due to neoclassical damping.

Figure 7 shows the "damping effectiveness" of an externally applied squeeze potential represented by coefficient a_2 plotted against temperature. The magnitude of a_2 changes by a factor of 20 over the range of temperature $5 \times 10^{-3}\mathrm{eV} < T < 0.5\mathrm{eV}$. The solid line is the theory prediction from Equation (218) of Ref. 11 in the range where the theory is applicable. According to theory, lowering the temperature below 0.1 eV moves the resonances in phase space to energies where the plasma is less populated (i.e., to higher phase velocities compared to the thermal velocity), therefore reducing the damping rate. For temperatures below 0.014 eV, bounce harmonic Landau damping is not applicable since the particles diffuse from one end of the plasma to

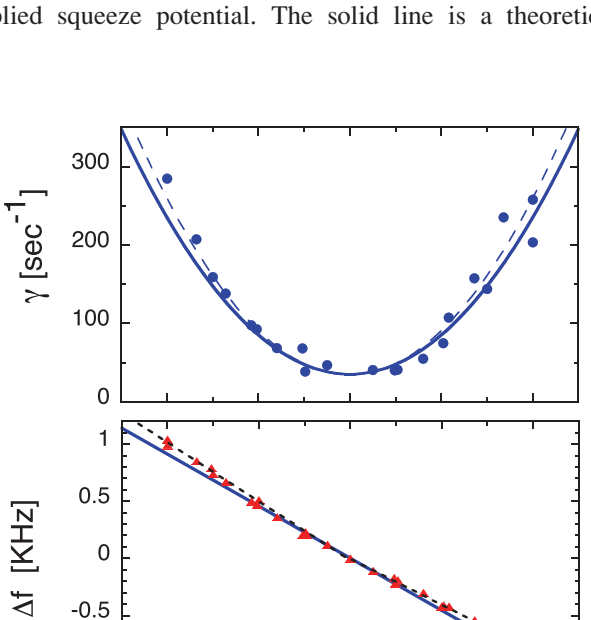

FIG. 5. Damping and frequency shift for both positive and negative squeeze voltages. Solid lines are theory predictions from Ref. 11, and the dashed line are fits to the data.

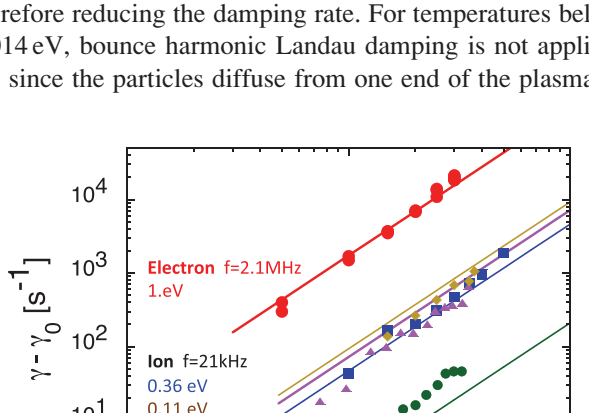

FIG. 6. Damping vs squeeze voltage for various plasmas, note that squeeze voltages are negative for electron plasma. Solid lines are theory predictions from Ref. 11.

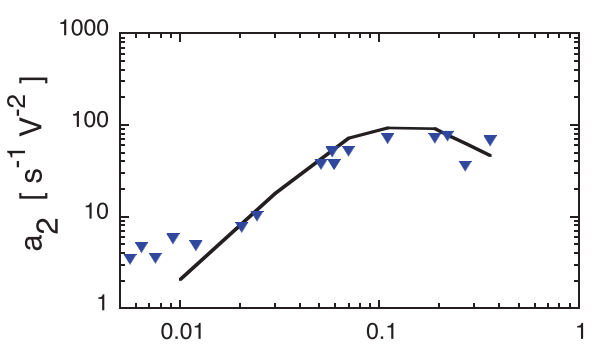

FIG. 7. Squeeze damping effectiveness vs temperature. Solid line is the theory prediction from Ref. 11.

the other instead of bouncing. At low temperatures, we observe weak damping not explain by bounce harmonic Landau damping, possibly due to neoclassical damping also scaling as V_s^2.

Landau damping results in a modification of the velocity distribution at the wave-particle resonant velocity. Using Coherent Laser Induced Fluorescence (LIF) techniques,[17] we are able to measure the wave coherent velocity distribution function, and thus directly determine the resonant particle velocity by looking for deviation from Maxwellian. With our knowledge of the plasma length and wave frequency, we are able to identify the spatial harmonic that causes this wave-particle resonance. Here, we excite a large amplitude wave in order to collect data during 50 ms in the presence of a significant amplitude wave. During the 50 ms averaging used for coherent LIF measurements, the wave amplitude $\mathcal{A}$ decayed by a factor of 3.27 due to squeezed damping of the wave. This is accounted for in analyzing the data by weighting δF in each phase-box data by $\mathcal{A}^{-1}$. Magnesium has 3 natural isotopes (Mg_{24}, 79%, Mg_{25}, 10%, and Mg_{26}, 11%). The 25 and 26 magnesium ion resonance frequencies are shifted by 2.28 GHz and 3.08 GHz, respectively. In each phase-box, the magnesium minority isotopes (25 and 26) have been removed according to their natural abundance, in order to display the particle velocity distribution, not merely the intensity of the fluorescence versus the laser wavelength.

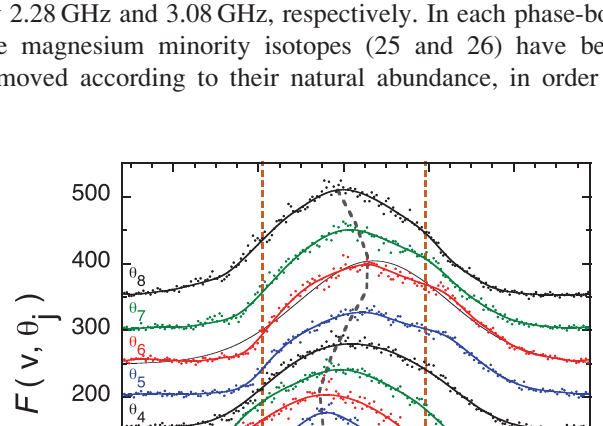

FIG. 8. Coherent particles distributions shown for 8 phases, each phase is offset vertically for clarity.

Figure 8 displays 8 phases-boxes of the coherently measured velocity distribution; the units are photons per millisecond per milliwatt of laser power. The entire distribution oscillates in the presence of a Trivelpiece Gould (TG) wave; the center of the particle distribution of each phase is marked by the wavy dashed line. Note that the phase velocity of $m_z = 1$ is located well outside the particles velocity distribution at $v_{ph} = 5{,}740$ m/s, causing Landau damping to be small. Furthermore, at large wave amplitudes, Landau damping is reduced by particle trapping at the phase velocity.[18] The center of the distribution exhibits an oscillation velocity of $v_0 = 584\,\mathrm{m/s} \times \cos(2\pi ft)$, where $f \simeq 21.95$ kHz. The peak velocity can also be written in term of $\bar{v}$ as $v_0 = 0.33\,\bar{v} \times \cos(2\pi ft)$ corresponding to $\delta n_0/n_0 = v_0/v_{ph} = v_0/(2fL_p) = 10\%$. It is worth noting that a $m_z = 1$ standing wave has a maximum δv in the center of the plasma, but in absence of squeeze no measurable δn at $z = 0$. That is the mode velocity is large on center and the density perturbation is large at the end of the column.

Figure 8 also shows distortion of the distribution around $v_{ph}/3$ marked by the dashed lines. Phase 6 has a Maxwellian curve plotted on top of the data to allow the eyes to see the distortion better. This distortion is due to the lowest-order bounce harmonic introduced by the squeeze potential. To analyze this perturbation better, we consider the normalized wave-coherent fluctuation $\delta F^{coh}(v)/F_0(v)$. Assuming a sinusoidal oscillation of $F(v)$, we analyze the amplitude and phase of the coherent motion as a function of v. The normalized coherent signal is

$$\frac{\delta F^{coh}(v)}{F_0(v)} \equiv \frac{\sum_{j=1}^{n\,phase} F(v,\theta_j) \times e^{i(\theta_j - \theta_0)}}{F_0(v)}, \tag{11}$$

where θ is the wave phase at which the distribution is measured. The particle response at each velocity $\delta F^{coh}(v)/F_0(v)$ has an amplitude and a phase, and here, we separate the response into a symmetric and an anti-symmetric parts. The velocity anti-symmetric particle response calculated from the coherently measured particle distribution $\delta F(v)/F_0(v)$ as

$$A(v) \equiv \frac{1}{2}\left(\frac{\delta F^{coh}(v)}{F_0(v)} - \frac{\delta F^{coh}(-v)}{F_0(-v)}\right), \tag{12}$$

and the velocity symmetric response as

$$S(v) \equiv \frac{1}{2}\left(\frac{\delta F^{coh}(v)}{F_0(v)} + \frac{\delta F^{coh}(-v)}{F_0(-v)}\right). \tag{13}$$

An advantage of looking at the symmetric and anti-symmetric response is that the symmetric response represents changes in the plasma density or temperature, and the anti-symmetric response represents the fluid velocity. The anti-symmetric response $A(v)$ and symmetric response $S(v)$ are plotted in Figure 9 for $F(v)$ measured at $z_L = 0$ and at radius $r_L = 0.4$ cm (open symbols). Also plotted is the

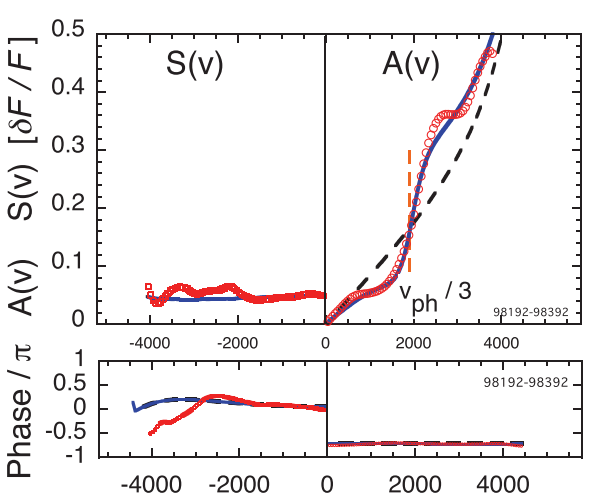

FIG. 9. Amplitude and phase of symmetric $S(v)$ and anti-symmetric $A(v)$ component of $\delta F(v)/F_0(v)$ in units of δF/F.

calculated response of a Maxwellian distribution shown with a dashed line. One sees that $A(v)$ deviates from the Maxwellian response, "crossing it" at one third of the phase velocity of a TG wave $(v_{ph}/3)$ indicating that particles bouncing in the trap at $v_b = v_{ph}/3$ (with frequency $f_b = f_{TG}/3$) are resonant with the wave. Bounce harmonics Landau damping is seen here directly moving particles slower than $v_{ph}/3$ to larger velocities at the expense of the wave amplitude. The symmetric part $S(v)$ is small and uniform across all velocities when V_s is applied close, but not exactly, on the center of the plasma column. $S(v)$ represents a coherent density change. The phase of $A(v)$ is uniform across all velocities and is out of phase by a little bit more than $\pi/2$ with $S(v)$. In the absence of applied squeeze, the symmetric response $S(v)$ is zero to experimental accuracy, that is, no density change is measurable at $z_L = 0$.

The anti-symmetric particle response on top of the Maxwellian response can be modeled as

$$A(v) = H_m \frac{v(|v| - v^*)}{(|v| - v^*)^2 + \beta^2}, \tag{14}$$

where m represents the mth harmonic component; H_m is the amplitude and β represents broadening of the resonance due to wave damping, collisions, and plasma "sloshing." The model superimposed on the Maxwellian response is shown with a solid line in Figure 9. As we will discuss later, the velocity at which the response change sign is $v^* \simeq v_{ph}/3$. The amplitude of the third harmonic is $H_3 = 0.35 \times \delta F/F$, i.e., a 35% change in $\delta F(v)/F(v)$ around $v_{ph}/3$. For our central squeeze, for which we expect that only odd harmonics will be present, we observe that mainly harmonic 3 is playing an important role and it appears that higher order harmonics are small.

The amplitude of the 3rd bounce harmonic H_3 is plotted in Figure 10 as a function of the applied squeeze voltage V_s. The harmonic strength increases as V_s increases, but is not zero when the applied squeeze voltage is zero. We believe

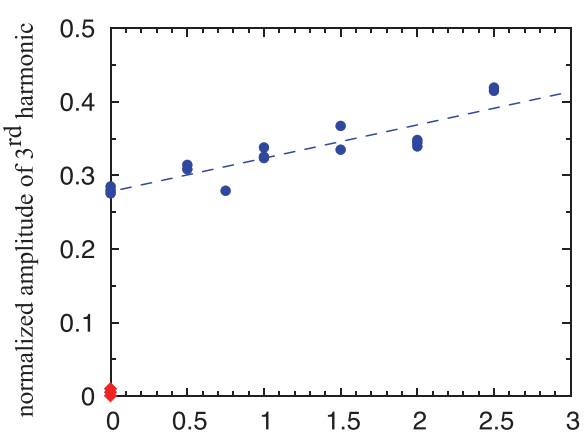

FIG. 10. Amplitude of 3rd spatial harmonic H_3 versus squeeze voltage.

that the harmonics at $V_s = 0$ are created by the plasma end effects. The axial confining potentials create rounded plasma ends. Rounded ends, in contrast to theoretical periodic boundaries conditions, introduce spatial harmonics. These end-effects can be turned off by "sloshing" the plasma at a non-resonant frequency (i.e., not a plasma mode). To "slosh" the plasma in the trap, we alternatively lower and raise the confining potential at each end of the plasma column at a low frequency compare to f_{TG}, effectively non-resonantly displacing the plasma and not creating any $k_z = m\pi/L_p$. Here, the measured displacement is in agreement with an oscillating Maxwellian, and the amplitude of the 3rd spatial harmonic is negligible as shown by the red diamond in Figure 10. The surprisingly large amount of third harmonic in the absence of squeeze $H_3(0)$ is not well understood at present. For large amplitude waves, Landau damping is reduced due to particle trapping, one may speculate that bounce harmonic Landau damping is less reduced for squeeze potential applied at the end of the plasma than on center.

Using a measured density profile $n_0(r, z_L)$, the potential applied on the electrodes, and presuming thermal equilibrium along a field line, one can calculate the potential inside

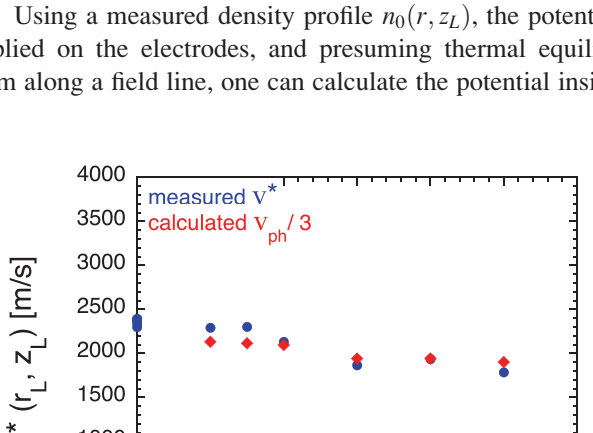

FIG. 11. Measured v^* compared to calculated $v_{ph}/3$.

the plasma $\varphi(r,z)$. The energy of a particle bouncing in the plasma is $E(r,z) = \frac{1}{2}mv^2(r,z) + e\varphi(r,z)$, and therefore, one can calculate the velocity of a particle at the location of the laser measurement $v(r_L, z_L)$ for one ion bouncing in the trap at $f_b = f_{TG}/3$. The calculated $v(r_L, z_L)$ are plotted in Figure 11 with diamonds, while the dots represent the location of measured v^*, demonstrating that the measured v^* correspond to particles bouncing at $f_b = f_{TG}/3$.

To summarize, the coherent $F(v)$ measurements clearly identify the third spatial harmonics with phase velocity $v_{ph}/3$ as playing a crucial role in the bounce harmonic Landau damping of plasma wave.

IV. DISCUSSION

Our results indicate that the observed squeezed damping is in quantitative agreement with the bounce harmonic Landau damping theory developed in Ref. 11. The theory describes particles with orbits perturbed but not trapped by the squeeze potential, moving in z and experiencing a non-sinusoidal mode potential. Our measurements confirm the existence of higher order spatial modes in the presence of squeeze potential or rounded ends. These measurements quantify squeeze damping and can be used also to set a limit on wave damping from the effect of spatial variations due to end effects and trap imperfections. Large amplitude waves allow us to see clearly the effects of particle bouncing at $f_b = f_{TG}/3$, but the magnitude of the bounce harmonics due to background squeeze is ill understood for large amplitude waves.

ACKNOWLEDGMENTS

This work was supported by the National Science Foundation Grant No. PHY-1414570, Department of Energy Grant No. DE-SC0002451and Department of Energy High Energy Density Laboratory Plasma Grant No. DE-SC0008693.

[1]H. L. Berk and D. L. Book, Phy. Fluids **12**, 649 (1969).
[2]A. N. Kaufman and T. Nakayama, Phys. Fluids **13**, 956 (1970).
[3]V. L. Karpman, B. I. Meerson, A. B. Mikkhailovsky, and O. A. Pokhotelov, Planet Space Sci. **25**, 573 (1977).
[4]B. I. Meerson, P. V. Sasorov, and A. V. Stepanov, Sol. Phys. **58**, 165 (1978).
[5]W. M. Sharp, H. L. Berk, and C. E. Nielsen, Phys. Fluids **22**, 1975 (1979).
[6]M. Koepke, R. F. Ellis, R. P. Majeski, and M. J. McCarrick, Phys. Rev. Lett. **56**, 1256 (1986).
[7]N. I. Grishanov, A. G. Elfimov, C. A. de Azevedo, and A. S. de Assis, Phys. Plasmas **3**, 3798–3808 (1996).
[8]B. P. Cluggish, J. R. Danielson, and C. F. Driscoll, Phys. Rev. Lett. **81**, 353 (1998).
[9]O. V. Polomarov, C. E. Theodosiou, and I. D. Kaganovich, Phys. Plasmas **12**, 080704 (2005).
[10]A. A. Kabantsev and C. F. Driscoll, Phys. Rev. Lett. **97**, 095001 (2006).
[11]A. Ashourvan and D. H. E. Dubin, Phys. Plasmas **21**, 052109 (2014).
[12]A. W. Trivelpiece and R. W. Gould, J. Appl. Phys. **30**, 1784–1793 (1959).
[13]S. A. Prasad and T. M. O'Neil, Phys. Fluids **26**, 665 (1983).
[14]F. Anderegg, X.-P. Huang, E. Sarid, and C. F. Driscoll, Rev. Sci. Instrum. **68**, 2367 (1997).
[15]X.-P. Huang, F. Anderegg, E. M. Hollmann, C. F. Driscoll, and T. M. O'Neil, Phys. Rev. Lett. **78**, 875 (1997); E. M. Hollmann, F. Anderegg, and C. F. Driscoll, Phys. Plasmas **7**, 2776 (2000).
[16]D. H. E. Dubin, Phys. Plasmas **21**, 052108 (2014).
[17]F. Anderegg, C. F. Driscoll, D. H. E. Dubin, and T. M. O'Neil, Phys. Rev. Lett. **102**, 095001 (2009).
[18]J. R. Danielson, F. Anderegg, and C. F. Driscoll, Phys. Rev. Lett. **92**, 245003 (2004).